Coulomb effects on the quantum transport of a two-dimensional electron system in periodic electric and magnetic fields

Andrei Manolescu
Institutul de Fizica şi Tehnologia Materialelor, Căsuţa Poştală MG-7 Bucureşti-Măgurele, Romania

Rolf R. Gerhardts
Max-Planck-Institut für Festkörperforschung, Heisenbergstrasse 1, D-70569 Stuttgart, Federal Republic of Germany
(Received 24 January 1997)

The magnetoresistivity tensor of an interacting two-dimensional electron system with a lateral and unidirectional electric or magnetic modulation, in a perpendicular quantizing magnetic field, is calculated within the Kubo formalism. The influence of the spin splitting of the Landau bands and of the density of states (DOS) on the internal structure of the Shubnikov–de Haas oscillations is analyzed. The Coulomb electron-electron interaction is responsible for strong screening and exchange effects and is taken into account in a screened Hartree-Fock approximation, in which the exchange contribution is calculated self-consistently with the DOS at the Fermi level. This approximation describes both the exchange enhancement of the spin splitting and the formation of compressible edge strips, unlike the simpler Hartree and Hartree-Fock approximations, which yield either one or the other. [S0163-1829(97)00740-6]

I. INTRODUCTION

Modern techniques allow the fabrication of semiconductor heterostructures incorporating a two-dimensional electron gas (2DEG) and a lateral periodic electrostatic potential (electric modulation) and/or a periodic magnetic field (magnetic modulation). In the presence of an external, constant, and perpendicular magnetic field, the modulation lifts the degeneracy of the Landau levels. The resulting Landau-band structure determines various oscillations of the magnetoresistivities, which usually provide the only accessible information on the modulation strength.

There are at least three types of modulation effects on the magnetoresistivities. First, the Weiss commensurability oscillations in the quasiclassical regime of low magnetic fields, both for the electric,[1] and, more recently for the magnetic modulations,[2,3] have attracted most of the experimental and theoretical work.[4,5] Second, the peculiar subband structure generated by a two-dimensional superlattice, known as the Hofstadter butterfly, leads to another type of commensurability oscillations, inside the Shubnikov–de Haas (SdH) peaks, their observation being currently the aim of important efforts.[6] Third, at high magnetic fields, the profile of the density of states (DOS) associated to the energy dispersion of the Landau bands, together with the exchange-enhanced spin splitting, may also determine an internal structure of the SdH maxima. In the present paper we will discuss only this last type of effects.

The experimental results have been obtained for the resistivity ρ_{xx} of GaAs-$Al_xGa_{1-x}As$ interfaces with an electric modulation in the x direction, i.e., of a one-dimensional character. The first investigation was performed on a modulation created by holographic illumination.[7] In the absence of the modulation the spin splitting of the second Landau level, with $n=1$, could not be resolved in the magnetoresistivity, but with increasing the modulation amplitude, the evolution of a double-peak structure was observed, and it was attributed to the van Hove singularities (vHS's) of the DOS.

Further experiments, on higher mobility samples modulated by etching techniques, have clearly shown the spin splitting. For a weak modulation, again, a double-peak and also a more complicated triple-peak structure have been detected in the spin-polarized SdH maxima of ρ_{xx} corresponding to the band $n=1$.[8] For a stronger modulation the spin splitting vanishes, but the magnetoresistivity *minima* at low even filling factors change into *maxima* at higher even filling factors, simultaneously with the shift of the minima towards the odd filling factors.[9] This behavior has convincingly been explained by the cumulated effects of the overlapping vHS's from adjacent Landau bands. In the experiments mentioned so far the modulation period has been in the range of 300–500 nm, and much larger than the magnetic length.

Another series of recent measurements has been performed on modulated systems produced by growing on vicinal surfaces.[10] This technique generates an electric modulation of a much shorter period, about 30 nm. The resistivity ρ_{xx} also displays a multipeak structure which may be related to the vHS's. The anisotropy of the resistivity, as well as an abrupt onset of the spin splitting for a high magnetic field, have been clearly shown.[11]

In all these experiments a detailed interpretation of the results is difficult, and still insufficiently clear. Beyond the technological constrictions, the difficulties arise from the complicated relationship between the DOS and the magnetoresistivities, and from the non-negligible electron-electron interaction effects. Therefore, a transport calculation combining on the same footing the electron-modulation, electron-electron, and electron-impurity interactions, and also thermal effects, is needed.

The anisotropy of the modulation may result in a high anisotropy of the conductivity tensor. The conductivity σ_{xx} has a scattering component (inter-Landau-level), which depends quadratically on the DOS and *vanishes* in the absence of the impurities. The conductivity σ_{yy} has an additional

band component (intra-Landau-level), determined by the dispersion of the one-particle energies, which *diverges* for weak electron-impurity collision broadening.[12] Therefore, in a high-mobility system, the band conductivity may cover the DOS effects in σ_{yy} and in the related resistivity ρ_{xx}.[13]

The Coulomb interaction also yields opposite effects. The tendency of the electrostatic screening is to reduce the energy dispersion imposed by the modulation on the effective single-particle states, and hence to *increase* the DOS. At the same time, the exchange interaction lowers the energy of the occupied states, enhances the energy gaps, but also broadens the Landau bands, *decreasing* the DOS. We have recently calculated the energy spectra[14] and the resistivity tensor[8] for a modulated system, in the Hartree-Fock approximation (HFA), and we could explain the spin splitting observed in the magnetotransport experiments. However, other exchange effects have been overestimated in the standard HFA.

The main artifact in the HFA results has been the appearance of strong short-range charge-density oscillations in the presence of a weak external modulation of period much longer than the magnetic length, for any filling factor. The reason is the competition of the Hartree interaction, of a repulsive character, with the Fock interaction, of an attractive character, which in the presence of the modulation may excite high charge-density harmonics.[15] This is reminiscent of the fact that the HFA predicts an instability of the homogeneous 2DEG against the formation of a charge-density wave for any filling factor,[16] whereas experiments indicate an inhomogeneous ground state (Wigner crystal) only for very low filling factors. Another consequence of the strong exchange energy is a strong exchange broadening of the Landau levels. A related implication is a substantial, qualitative contradiction between the HFA and the results of the Hartree[17,18] or Thomas-Fermi calculations[19] of edge states. While the latter predict compressible edge strips much wider than the magnetic length, but only the bare spin splitting (which is negligible for GaAs), the HFA gives considerably narrower compressible edge channels, but a strong splitting.[20–22,14] However, the experimental confirmation of wide edge channels[23] suggests the domination of the electrostatic effects.

In order to avoid, or at least to minimize, these artificial features of the HFA, our previous attempt to include the Coulomb interaction in a magnetotransport calculation for modulated systems has been limited to short modulation periods.[8] The steepness of the energy dispersion, on the magnetic length scale, can reduce the relative importance of the exchange interaction, such that the HFA may become qualitatively reasonable.

In the present paper we want to extend our calculations to the situation when the modulation period is much longer than the magnetic length. Therefore our efforts will be mainly focussed on the electron-electron interaction. Some preliminary results have already been reported.[24] Our approach is based on a screened HFA (SHFA), in which we include the influence of screening on the exchange interaction. Although we consider only static screening, this already leads to the desired reduction of the exchange effects and avoids the artifacts of the bare HFA. The screening is mainly determined by the DOS at the Fermi level.[25] Therefore, when the latter will be in an energy gap, the screening will be weak, such that the exchange enhancement of the Zeeman splitting will remain essentially like in the HFA. However, when the Fermi level will intersect a Landau band, the exchange effects will substantially diminish.

The Coulomb interaction is included in a transport calculation, within the standard Kubo formalism. For this purpose we need to consider an electron-impurity scattering mechanism. We will describe it within a self-consistent Born approximation (SCBA).

The realization of a magnetic modulation with a period of a few hundred nanometers, and a large amplitude, of the order of 1 T is technically feasible.[26] In the presence of a constant external magnetic field such a modulation will produce Landau bands and a charge-density response. Hence screening and exchange effects will occur, as for an electric modulation. Even in the absence of relevant magetotransport measurements, we will include in our calculation such a periodic magnetic field. For simplicity we will discuss only the case when the modulation, electric or magnetic, is unidirectional and sinusoidal.

The paper is organized as follows. In Sec. II we derive the self-consistent equations of the SHFA which give us the ground state of the system. Then, in Sec. III, we discuss the impurity scattering and the conductivity tensor. The numerical results of the transport calculation are presented in Sec. IV, and the conclusions are collected in Sec. V. Some technical details are given in two Appendixes.

II. SCREENED HARTREE-FOCK APPROXIMATION

We combine the influence of the electron-electron and the electron-impurity interactions on the single-particle states of the modulated 2DEG with the help of the average Green function, having the operatorial definition

$$G(E)\equiv\langle\hat{G}^{-}(E)\rangle_{\mathrm{imp}}=\frac{1}{E-[H^{0}+\Sigma^{\mathrm{ee}}+\Sigma^{\mathrm{ei}}(E)]}, \quad (2.1)$$

with the following notations: $\langle\cdots\rangle_{\mathrm{imp}}$ stands for the average over all the impurity configurations; $\hat{G}^{\pm}(E)=(E-H\pm i0^{+})^{-1}$, with H a generic one-body Hamiltonian of the interacting 2DEG with impurities; H^{0} is the Hamiltonian of the noninteracting 2DEG without impurities; Σ^{ee} and Σ^{ei} are the self-energy operators determined by the electron-electron and electron-impurity interactions, respectively.

In our case the noninteracting Hamiltonian has the form

$$H^{0}=\frac{1}{2m^{*}}[\mathbf{p}+e\mathbf{A}(\mathbf{r})]^{2}+V\cos Kx-\frac{\sigma}{2}g\mu_{B}B(x). \quad (2.2)$$

The electrons are located in the plane $\{\mathbf{r}=(x,y)\}$. $B(x)$ is the projection of the magnetic field along the z axis, and it may have a periodic component, $B(x)=B_{0}+B_{1}\cos Kx$, similar to the periodic electrostatic potential $V(x)=V\cos Kx$. We choose the vector potential in the Landau gauge, as imposed by the symmetry of our system,

$$\mathbf{A}(\mathbf{r})=\left(0,B_{0}x+\frac{B_{1}}{K}\sin Kx\right). \quad (2.3)$$

We have also included in H^0 the Zeeman term, where $\sigma=+$ for spin-up and $\sigma=-$ for spin-down states, g is the bare, band structure g factor, and μ_B the Bohr magneton.

We use the eigenfunctions of H^0 corresponding to the unmodulated system, i.e., for $B_1=0$ and $V=0$, as the basis for the one-particle Hilbert space. These functions are the well-known Landau wave functions, $f_{nX_0}(x,y)=L_y^{-1/2}\exp(-iX_0y/l^2)f_{nX_0}(x)$, where $f_{nX_0}(x)$ are the one-dimensional harmonic-oscillator wave functions, with $n=0,1,\ldots$, centered at the position X_0, called the center coordinate. Here l is the magnetic length, and we will denote by ω_c the cyclotron frequency, both corresponding to the *uniform* component of the magnetic field B_0, $l=(\hbar/eB_0)^{1/2}$ and $\omega_c=eB_0/m^*$. In order to simplify the notations we keep the same symbol for the two-variable wave function which depends on both spatial coordinates x and y, e.g., $f_{nX_0}(x,y)$, and for the reduced wave function depending only on x, $f_{nX_0}(x)$. The distinction will be made by the number of variables specified inside the brackets. The plane-wave factor has been normalized to the macroscopic length L_y. The matrix elements of H^0 are given in Appendix A.

We will assume randomly distributed impurities, such that the modulated system is invariant to translations along the y axis. Consequently, the dependence on y of the interacting, effective, one-particle wave functions, also factorizes in a simple plane wave. For these wave functions we use the notation $\psi_{n\sigma X_0}(x,y)=L_y^{-1/2}\exp(-iX_0y/l^2)\psi_{n\sigma X_0}(x)$, and we expand them in the Landau basis,

$$\psi_{n\sigma X_0}(x)=\sum_{n'} c_{nn'}(\sigma,X_0)f_{n'X_0}(x). \tag{2.4}$$

For the interacting, unmodulated system, we have $c_{nn'}(\sigma,X_0)=\delta_{nn'}$, and the dependence on the spin label arises as long as the exchange interaction and an external modulation are simultaneously present. The periodic fields broaden the degenerate Landau levels $E_{n\sigma}$ into energy bands, $E_{n\sigma X_0}$, which we find by solving the eigenvalue problem

$$(H^0+\Sigma^{\rm ee})\psi_{n\sigma X_0}(x,y)=E_{n\sigma X_0}\psi_{n\sigma X_0}(x,y). \tag{2.5}$$

The averaged effect of the impurities consists in the spreading of the effective single-particle energies around the energy spectrum given by Eq. (2.5), and thus in an additional energy broadening. The statistical weight of an arbitrary energy E is given by the spectral function,

$$\rho_{n\sigma X_0}(E)=\frac{1}{\pi}\mathrm{Im}\langle\psi_{n\sigma X_0}|G(E)|\psi_{n\sigma X_0}\rangle, \tag{2.6}$$

and the contribution of the effective state $(n\sigma X_0)$ to the filling factor ν can be defined as

$$\nu_{n\sigma X_0}=\int dE\,\rho_{n\sigma X_0}(E)\mathcal{F}(E), \tag{2.7}$$

$\mathcal{F}(E)=[\exp(E-\mu)/T+1]^{-1}$ being the Fermi function, with μ the chemical potential and T the temperature, such that

$$\nu=\sum_{n\sigma}\int_0^a\frac{dX_0}{a}\nu_{n\sigma X_0}. \tag{2.8}$$

We will discuss the electron-impurity interaction model in Sec. III. Clearly, in the absence of the impurities $\rho_{n\sigma X_0}(E)\equiv\delta(E-E_{n\sigma X_0})$.

For calculating the electron-electron self-energy we start with the form given by the HFA.[27,28] In the Landau basis the matrix elements $\Sigma^{\rm ee}_{n\sigma X_0,n'\sigma' X_0'}$ do not mix the spin and the center-coordinate quantum numbers, and can be written as

$$\begin{aligned}\Sigma^{\rm ee}_{nn'}(\sigma,X_0)=&\sum_{m\tau Y_0}\nu_{m\tau Y_0}\int\\&\times d\mathbf{r}\,d\mathbf{r}'f^*_{nX_0}(x,y)\psi^*_{m\tau Y_0}(x',y')u(\mathbf{r}-\mathbf{r}')\\&\times[f_{n'X_0}(x,y)\psi_{m\tau Y_0}(x',y')\\&-\delta_{\sigma\tau}f_{n'X_0}(x',y')\psi_{m\tau Y_0}(x,y)]\\\equiv&\Sigma^{{\rm ee},H}_{nn'}(X_0)+\Sigma^{{\rm ee},F}_{nn'}(\sigma,X_0),\end{aligned} \tag{2.9}$$

where $u(\mathbf{r})=e^2/(\kappa|\mathbf{r}|)$ is the Coulomb potential with κ the dielectric constant of the semiconductor background. The two terms in the square brackets of Eq. (2.9) define the Hartree (direct) and the Fock (exchange) contributions, indicated by the superscripts H and F. The Hartree term can be rewritten in terms of the particle density,

$$n(x)=\sum_{m\tau Y_0}\nu_{m\tau Y_0}|\psi_{m\tau Y_0}(x)|^2=\sum_{p\geq 0}n_p\cos pKx, \tag{2.10}$$

the last form being the Fourier expansion appropriate to our external fields. The Fourier coefficients of the Hartree self-energy are given in Appendix A.

Using Eq. (2.4) and the Fourier transform of the Coulomb potential, $\tilde{u}(\mathbf{q})=2\pi e^2/(\kappa|\mathbf{q}|)$, the Fock self-energy becomes

$$\begin{aligned}\Sigma^{{\rm ee},F}_{nn'}(\sigma,X_0)=&-\sum_{mY_0}\nu_{m\sigma Y_0}\sum_{m_1m_2}c_{mm_1}(\sigma,Y_0)c_{mm_2}(\sigma,Y_0)\\&\times\int\frac{d\mathbf{q}}{(2\pi)^2}\tilde{u}(\mathbf{q})\langle f_{nX_0}|e^{i\mathbf{qr}}|f_{m_1Y_0}\rangle\\&\times\langle f_{m_2Y_0}|e^{-i\mathbf{qr}}|f_{n'X_0}\rangle.\end{aligned} \tag{2.11}$$

The Fourier expansion of $\Sigma^{{\rm ee},F}_{nn'}(\sigma,X_0)$ is also given in Appendix A.

In order to overcome the artifacts of the HFA mentioned in Sec. I, we screen the Coulomb potential in the exchange self-energy, substituting $\tilde{u}(\mathbf{q})$ in Eq. (2.11) by

$$\tilde{u}(\mathbf{q})=\frac{e^2}{\kappa}\frac{2\pi}{q\epsilon(q)}, \tag{2.12}$$

where $\epsilon(q)$ is the *static* dielectric function. We thus neglect the dynamic screening effects. In the spirit of the random-phase approximation, $\epsilon(q)=1-(2\pi e^2/\kappa q)\chi(q)$, $\chi(q)$ being the dielectric susceptibility given by the well-known Lindhard formula,[27] to be evaluated self-consistently with the effective states resulting from Eq. (2.5). In the diagrammatic picture, Fig. 1, that means the series of the polarization

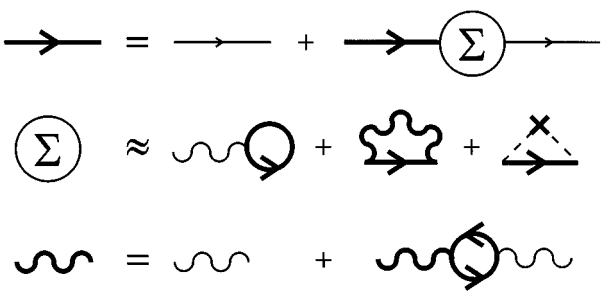

FIG. 1. Diagrammatic representation of the combined screened Hartree-Fock and self-consistent Born approximations. The wavy lines are the Coulomb interaction and the dashed line is the electron-impurity interaction.

loops—previously contained only in the Hartree part of Σ^{ee}—is now included, via Eq. (2.12), also in the Fock part.

For a two-dimensional system in a perpendicular magnetic field, one can identify two components of the static dielectric susceptibility,

$$\chi(q)=\chi_1(q)+\chi_2(q), \tag{2.13}$$

corresponding to the *intra*- and to the *inter*-Landau-level transitions, respectively.[29] In other words, $\chi_1(q)$ describes the electrostatic response due to the electron redistribution around the Fermi level, under the action of an electric field of an arbitrary wave vector $\mathbf{q}$, while $\chi_2(q)$ gives the response due to the distortion of the effective wave functions.

For χ_1 we use the expression derived for *homogeneous* systems by Labbé,[30] which we average over the Brillouin zone determined by the external electric or magnetic modulation:

$$\chi_1(q)=\frac{-1}{2\pi l^2}\sum_{n\sigma}\int_0^a \frac{dX_0}{a}\frac{\partial \nu_{n\sigma X_0}}{\partial \mu}\left[F_{nn}\left(\frac{(ql)^2}{2}\right)\right]^2, \tag{2.14}$$

where we have used Eq. (A1). We expect that this approximation is appropriate for weakly modulated systems characterized by $lV \ll a\hbar\omega_c$, or $lB_1 \ll aB_0$. Within the same procedure we evaluate χ_2 as[29]

$$\chi_2(q)=\frac{1}{2\pi l^2}\sum_{n\neq n'}\left[F_{nn'}\left(\frac{(ql)^2}{2}\right)\right]^2 \times\sum_{\sigma}\int_0^a \frac{dX_0}{a}\frac{\nu_{n\sigma X_0}-\nu_{n'\sigma X_0}}{E_{n\sigma X_0}-E_{n'\sigma X_0}}. \tag{2.15}$$

For a sufficiently high magnetic field B_0, that is for sufficiently large energy gaps $E_{n+1,\sigma X_0}-E_{n\sigma X_0}$, and for a small q, $\chi_2(q)$ is typically negligible with respect to $\chi_1(q)$, except eventually when there are very few states at the Fermi level such that $\chi_1(q)$ is vanishingly small. Since for our weak modulations, in the limit $q\to 0$, $\chi_1(q)$ becomes proportional to the thermodynamic DOS, i.e., $\partial n/\partial\mu$, we can say the screening of the exchange interaction is dominated by the intra-Landau-level transitions, which at low temperatures are determined by the DOS at the Fermi level.

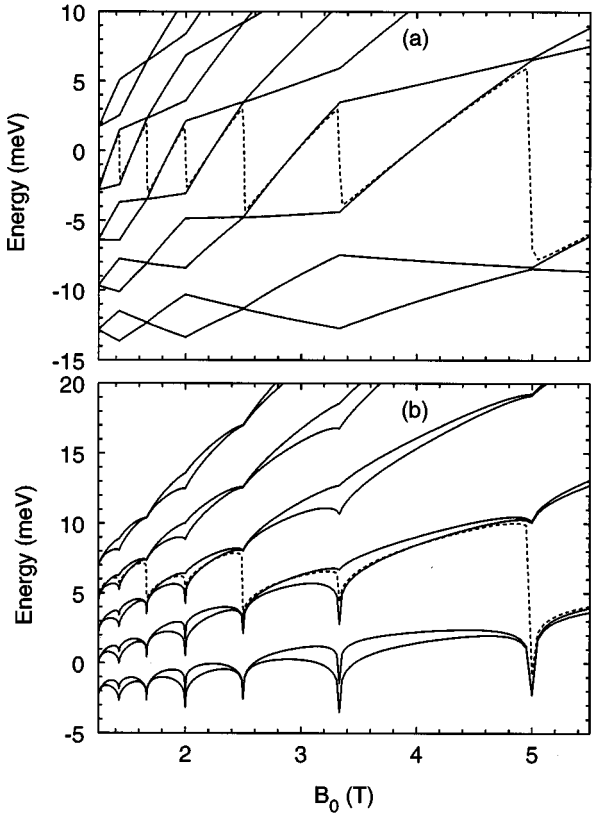

FIG. 2. The Landau fan (a) in the HFA and (b) in the SHFA for a homogeneous GaAs system. The dashed line shows the chemical potential. The temperature $T=1$ K.

This SHFA has been used in the papers by Ando, Ohkawa, and Uemura for explaining the exchange enhancement of the Zeeman[31] and of the valley splitting[32] in homogeneous Si metal-oxide-semiconductor systems. Further improvements have incorporated the dynamic screening, within the plasmon-pole approximation, and the Coulomb-hole correlation effects, for the calculation of the photoluminescence energy in n-doped GaAs quantum wells.[33,34] Nevertheless, in order to keep the consistent treatment of ground-state and transport properties tractable, we will neglect such additional corrections in the study of the modulated systems. In particular, even without dynamic screening effects, our results for the self-energy for a homogeneous 2DEG in a GaAs-$Al_xGa_{1-x}As$ interface are qualitatively similar to those shown in Refs. 33 and 34. In Fig. 2 we compare the first five spin splitted Landau levels vs magnetic field, i.e., the Landau fan, in the standard (bare) HFA with the results given by the SHFA. The material parameters are $m^*=0.067m_0$, $g=0.4$, and $\kappa=12.7$, and the carrier concentration is chosen such that $\nu B_0=10$ T, ν being the filling factor. Both the Landau and the spin gaps are enhanced by the exchange interaction, but in the SHFA the Fock self-energy is strongly dependent on the DOS at the Fermi level, $D(E_F)$. Thus the exchange interaction is screened for a high $D(E_F)$, i.e., for noninteger filling factors, but it may become very large for an integer filling. Since the exchange interaction is negative, the screening mechanism leads to the deep cusps in Fig. 2(b), also present in the dynamic-screening calculations.[33,34] As in the HFA, the largest energy gaps occur for integer filling factors.

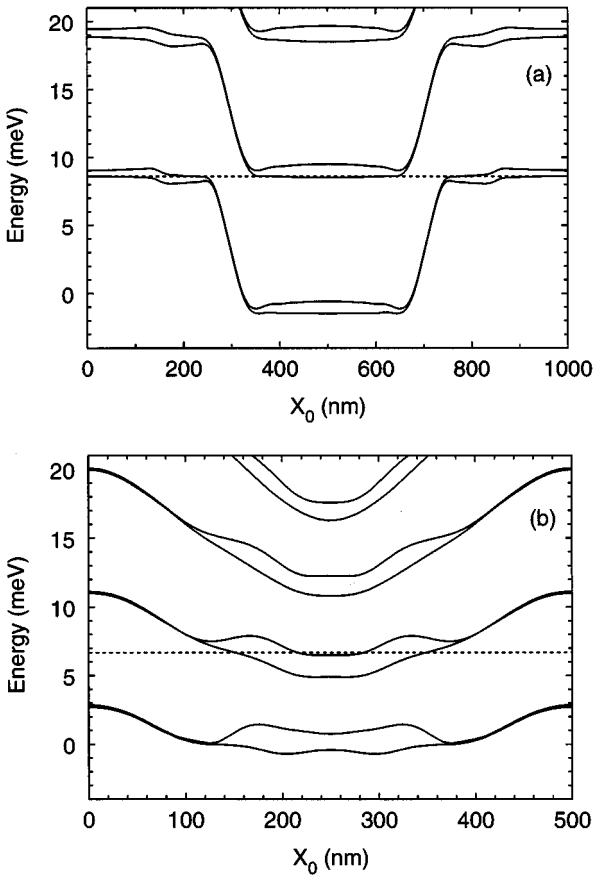

FIG. 3. Compressible and incompressible strips in the SHFA, for (a) an electric modulation having $a=1000$ nm and $V=200$ meV with $B_0=6$ T, and (b) a magnetic modulation having $a=500$ nm and $B_1=1.2$ T and $B_0=4$ T. The Fermi level is indicated by the horizontal dashed line. $T=1$ K.

The thermal energy is much smaller than the energy gaps, and no disorder broadening is assumed. Therefore the gaps at integer filling factors in Fig. 2(b) are smaller than those in Fig. 2(a), only because of the screening involved by the response of the wave functions, described by χ_2.

We believe that the energy spectra, which we obtained within the SHFA for the modulated system, are much improved with respect to those in the HFA. In Fig. 3(a) we show the SHFA of the Landau bands generated by an electric modulation of a period much larger than the magnetic length. The Zeeman splitting is enhanced in the states around the Fermi energy, with replica in each of the upper and lower Landau bands, as in the HFA.[14] The improvement consists in the recovering of the pinning effect, resulting from electrostatic screening,[25] on the spin-split energy bands near the Fermi level. The pinning effect defines both compressible (dispersionless) and spin-polarized strips. In the HFA, for the modulation parameters of Fig. 3(a), strong short-range oscillations of the effective energies and of the charge density, with typical periods of $3-5l$, would occur. Those oscillations would disappear only if the energy dispersion imposed by the external modulation would dominate the interaction effects, i.e., for a sufficiently short modulation period and/or for a sufficiently large modulation amplitude.[14] In sufficiently strong modulation or steep confinement potentials the exchange enhancement of spin splitting is suppressed. With a decreasing slope of the potential, the enhancement recovers suddenly, and a large spin splitting of the Landau bands occurs nearly symmetrically with respect to the Fermi energy in such a manner, that both spin polarized bands touch the Fermi energy with large dispersions. Thus the compressible strips obtained in the Hartree approximation are destroyed in the bare HFA and replaced with spin-polarized incompressible strips. This spin polarization of the edge states may occur spontaneously even if the bare g factor vanishes, and has been discussed as a type of phase transition.[20–22] We believe that the occurrence of this spontaneous spin polarization is an artifact of the unscreened HFA, since our SHFA yields (as long as $a \gg l$) only a very smooth and gradual reduction of the spin splitting with increasing modulation strength, with compressible spin-polarized strips (energies pinned to the Fermi energy) instead of incompressible ones.

In Fig. 3(b) we transpose the results shown in Fig. 3(a) for a magnetic modulation. In this case the Hartree (direct) screening is weaker, due to the weaker, purely quantum-mechanical, coupling of the charge density to the nonuniform magnetic field, and consequently the pinning effect is less pronounced in Fig. 3(b). The peculiar Hartree response to a nonuniform magnetic field, which becomes negligible in the classical limit (cyclotron radius at the Fermi energy larger than the modulation period) will be discussed in detail elsewhere.[35] In the present paper we restrict ourselves to a strong uniform component B_0, such that the electrostatic and the exchange effects due to the periodic component are similar to those due to the electric modulation.

III. CONDUCTIVITIES

In order to calculate conductivities we have to consider the electron-impurity interaction. For randomly distributed impurities, the self-energy $\Sigma^{\rm ei}$ is diagonal with respect to X_0, and obviously also with respect to σ. Since we are mostly interested in the effects due to the electron-electron interaction, we simplify the calculation of $\Sigma^{\rm ei}$ by employing the phenomenological ansatz in which one ignores the dependence of its matrix elements on the Landau quantum number n and on the center coordinate X_0, that is $\Sigma^{\rm ei}_{n\sigma X_0, n'\sigma X_0}(E) \approx \Sigma^{\rm ei}_{\sigma}(E)\,\delta_{nn'}$. In the SCBA, Fig. 1, we need to solve the equation[13]

$$\Sigma^{\rm ei}_{\sigma}(E) = \Gamma^2 \sum_n \int_0^a \frac{dX_0}{a} G_{n\sigma X_0}(E)$$

$$= \Gamma^2 \sum_n \int_0^a \frac{dX_0}{a} \frac{1}{E - E_{n\sigma X_0} - \Sigma^{\rm ei}_{\sigma}(E)}. \quad (3.1)$$

We also take a simple parametrization of the electron-impurity interaction energy, $\Gamma = \gamma\sqrt{B(\mathrm{T})}$ (meV). Using Eq. (3.1) the DOS can be written in the form

$$D(E) = \frac{\hbar\omega_c}{\pi\Gamma^2} D_0 \sum_{\sigma} \mathrm{Im}\,\Sigma^{\rm ei}_{\sigma}(E), \quad (3.2)$$

where $D_0 = m^*/2\pi\hbar^2$ is the DOS per spin level for the homogeneous system without magnetic field.

The standard Kubo formula for the conductivity tensor can be written as

$$\sigma_{\alpha\beta}(\omega)=e\int_0^\infty dt\,\frac{e^{i\omega t}-1}{\hbar\omega}e^{-\varepsilon t}\times\mathrm{Tr}\langle\mathcal{F}(H)[\dot{r}_\beta,e^{(i/\hbar)Ht}j_\alpha e^{-(i/\hbar)Ht}]\rangle_{\mathrm{imp}},\tag{3.3}$$

where $\alpha,\beta=x,y$, $r_\alpha\equiv\alpha$, and $\varepsilon\to0^+$. The operator $\dot{\mathbf{r}}$ is given by

$$\dot{\mathbf{r}}=\frac{i}{\hbar}[H,\mathbf{r}]\equiv\mathbf{v}^0+\mathbf{v}^{\mathrm{ex}},\tag{3.4}$$

where $\mathbf{v}^0$ is the usual form of the velocity operator, resulting from the commutator of the noninteracting Hamiltonian H^0, with the position

$$\mathbf{v}^0=\frac{1}{m^*}[\mathbf{p}+e\mathbf{A}(\mathbf{r})].\tag{3.5}$$

All the other terms of the full Hamiltonian H commute with $\mathbf{r}$ except the Fock self-energy, due to its nonlocal character. According to Eqs. (2.9) and (2.10), the Coulomb interaction gives an exchange contribution to the velocity operator of the form

$$\mathbf{v}^{\mathrm{ex}}=\frac{i}{\hbar}[\Sigma^{\mathrm{ee},F},\mathbf{r}].\tag{3.6}$$

The matrix elements of the velocity operators (3.5) and (3.6), in the Landau basis, can be found in Appendix B. For the current-density operator we adopt the definition

$$\mathbf{j}=-\frac{e}{L_xL_y}\,\dot{\mathbf{r}},\tag{3.7}$$

and we will call the term corresponding to Eq. (3.6) the ''exchange current.'' After a straightforward manipulation the Kubo formula can be put into the form

$$\sigma_{\alpha\beta}(\omega)=\frac{1}{i\omega}[\lambda_{\alpha\beta}(\omega)-\lambda_{\alpha\beta}(0)],\tag{3.8}$$

with

$$\lambda_{\alpha\beta}(\omega)=\frac{-e^2}{L_xL_y}\int_{-\infty}^{\infty}dE\,\mathcal{F}(E)\mathrm{Tr}\{\langle\delta(E-H)\dot{r}_\alpha\hat{G}^+(E+\hbar\omega)\dot{r}_\beta\rangle_{\mathrm{imp}}+\langle\dot{r}_\beta\hat{G}^-(E-\hbar\omega)\dot{r}_\alpha\delta(E-H)\rangle_{\mathrm{imp}}\}.\tag{3.9}$$

Of course $\dot{\mathbf{r}}$ depends on the impurity configuration, via the exchange contribution. However, since in the following we will restrict ourselves to a weak disorder, the dependence of Eq. (3.6) on the disorder broadening will be negligible. Therefore we neglect the impurity effects on $\dot{\mathbf{r}}$ in Eq. (3.9). Then, making use of the formal relation $\delta(E-H)=[\hat{G}^-(E)-\hat{G}^+(E)]/2\pi i$, we find that, in the static limit, $\omega\to0$, we have to average combinations like $\langle\hat{G}^\pm(E)\dot{r}_\alpha\hat{G}^\pm(E)\rangle_{\mathrm{imp}}$. The result can be written as

$$\langle\hat{G}^\pm(E)\dot{r}_\alpha\hat{G}^\pm(E)\rangle_{\mathrm{imp}}=-\frac{e}{L_xL_y}\langle\hat{G}^\pm(E)\rangle_{\mathrm{imp}}\times\left(\dot{r}_\alpha+\frac{i}{\hbar}[\Sigma^{\mathrm{ei}}(E),r_\alpha]\right)\times\langle\hat{G}^\pm(E)\rangle_{\mathrm{imp}},\tag{3.10}$$

where we have used a Ward identity to express the current vertex correction due to the impurities with the help of the corresponding self-energy operator.[36] Since we have assumed $\Sigma^{\mathrm{ei}}(E)$ to be a trivial (spin-dependent) c number, the impurity vertex correction vanishes. But we see that the Coulombian vertex correction is automatically included in Eq. (3.10) via the exchange current.

The Hall conductivity can now be written as[13]

$$\sigma_{xy}=-\sigma_{yx}=\frac{\hbar e^2}{i\pi^2l^2}\int_{-\infty}^{\infty}dE\,\mathcal{F}(E)\int_0^a\frac{dX_0}{a}\sum_{nn'\sigma}\langle\psi_{n\sigma X_0}|\dot{x}|\psi_{n'\sigma X_0}\rangle\times\langle\psi_{n'\sigma X_0}|\dot{y}|\psi_{n\sigma X_0}\rangle\mathrm{Im}\,G_{n\sigma X_0}(E)\mathrm{Re}\frac{d}{dE}G_{n'\sigma X_0}(E).\tag{3.11}$$

Since we treat the disorder in the SCBA, we cannot consider localization effects, and hence we cannot expect real Hall plateaus. Moreover, if the disorder broadening of the Landau levels is much smaller than the energy bands, Eq. (3.11) can be well approximated by the limit of a vanishing electron-impurity interaction, $\gamma\to0$. In this limit σ_{xy} takes the more familiar form

$$\sigma_{xy}=\frac{i\hbar e^2}{\pi l^2}\int_0^a\frac{dX_0}{a}\sum_{n\neq n',\sigma}\mathcal{F}(E_{n\sigma X_0})\times\frac{\langle\psi_{n\sigma X_0}|\dot{x}|\psi_{n'\sigma X_0}\rangle\langle\psi_{n'\sigma X_0}|\dot{y}|\psi_{n\sigma X_0}\rangle}{(E_{n\sigma X_0}-E_{n'\sigma X_0})^2},\tag{3.12}$$

in which the energy gaps are explicitly evidenced.

It is instructive to mention that, neglecting the exchange current, one obtains deviations from the well-known quantized values $\sigma_{xy}=(e^2/h)\times(\text{integer})$, for an integer filling factor. Let us consider the simplest case, with no external modulation. In the absence of the Coulomb interaction the energy gaps are determined by the cyclotron energy. The cyclotron frequency squared, in the denominator of Eq. (3.12), is compensated for by the cyclotron frequencies introduced in the numerator by the velocity matrix elements, Eq. (B1), and for a sufficiently low temperature one obtains the simple Drude formula $\sigma_{xy}=(e^2/h)\nu$. When the Coulomb interaction is present, the energy gaps are enhanced, but a similar enhancement occurs in the numerator, determined by the exchange term of the velocities, Eqs. (3.6) and (B3), and the Drude formula remains valid. Obviously, when the exchange interaction is screened, the exchange currents may be small. In our calculations, for the modulated systems, their contribution to the conductivities have been of the order 30–50 % in the HFA,[8] but of no more than 10% in the present SHFA.

The longitudinal conductivities can be transformed from Eqs. (3.8)–(3.9) to

$$\sigma_{\alpha\alpha}=\int dE\left(-\frac{d\mathcal{F}}{dE}\right)\sigma_{\alpha\alpha}(E), \tag{3.13}$$

$$\sigma_{\alpha\alpha}(E)=\frac{\hbar e^2}{l^2\pi^2}\int_0^a\frac{dX_0}{a}\sum_{nn'\sigma}|\langle\psi_{n\sigma X_0}|\dot{r}_\alpha|\psi_{n'\sigma X_0}\rangle|^2 \times \mathrm{Im}\,G_{n\sigma X_0}(E)\,\mathrm{Im}\,G_{n'\sigma X_0}(E).$$

The relation between the longitudinal conductivities and the DOS is complicated. Both the diagonal conductivities σ_{xx} and σ_{yy} have interlevel components, corresponding to $n\neq n'$ in Eq. (3.13), also known as *scattering* conductivities. One can show, by inspecting Eq. (3.13), that for a weak disorder, $\gamma\to 0$, the scattering conductivities become proportional to $[\Gamma D(E_F)]^2$. Hence they qualitatively reproduce the DOS profile, with van Hove singularities corresponding to the edges of the one-dimensional Landau bands.

Due to the anisotropy of the system, an intralevel component of Eq. (3.13), with $n=n'$, is nonzero for σ_{yy} only. It is called *band* conductivity,[12,13] being directly related to the dispersion of the Landau bands which yields equilibrium Hall currents. If the Hamiltonian is a local operator, the Hellman-Feynman theorem leads to

$$\frac{dE_{n\sigma X_0}}{dX_0}=-m\omega_c\langle\psi_{n\sigma X_0}|\dot{y}|\psi_{n\sigma X_0}\rangle, \tag{3.14}$$

which is no longer valid when the exchange interaction is considered. However, if the latter is screened, the deviations from Eq. (3.14) are not very important, and the band conductivity can still be understood in terms of the energy dispersion. Classically, it corresponds to the quasifree drift of the centers of the cyclotron orbits along the y axis, parallel to the periodic electric field. Thus the band conductivity behaves contrary to the scattering components: It vanishes at the band edges, has maxima at the band centers, and *diverges* for a small disorder, like γ^{-2}, becoming the dominant contribution to σ_{yy}.

The structure of the longitudinal conductivities, $\sigma_{xx}(E)=\sigma_{xx}^{\text{scattering}}(E)$ and $\sigma_{yy}(E)=\sigma_{yy}^{\text{scattering}}(E)+\sigma_{yy}^{\text{band}}(E)$, for an isolated, sinusoidal Landau band are qualitatively displayed in Fig. 4. In our calculations the two scattering conductivities are nearly equal. In Fig. 4(a) we assume a small band conductivity, such that both σ_{xx} and σ_{yy} show the two van Hove peaks. Reducing the disorder broadening the scattering components decrease, but at the same time the band conductivity increases, and a triple-peak structure evolves in σ_{yy}, Fig. 4(b), while the shape of σ_{xx} remains unchanged. For an even smaller disorder σ_{yy} becomes dominated by the band conductivity, the central peak covering the vHS, like in Fig. 4(c).

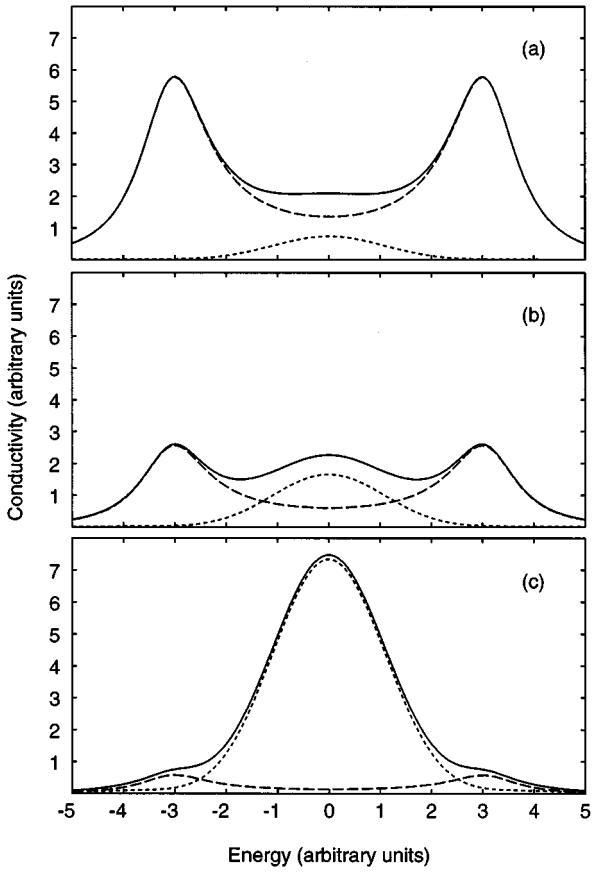

FIG. 4. Three possible profiles of the magnetoconductivity corresponding to a sinusoidal-like isolated Landau band. The full lines show σ_{yy}, the dashed lines show both σ_{xx} and the scattering component of σ_{yy}, and the dotted lines show the band conductivity.

IV. DISCUSSION OF THE NUMERICAL RESULTS

We perform the calculations of the effective electronic states within a numerical iterative scheme, starting from the noninteracting solution, and assuming a fixed number of particles for determining the chemical potential. At each step we diagonalize the Hamiltonian matrix, Eqs. (A2), (A9), and (A10), in L points of the half Brillouin zone, $0\leqslant X_0\leqslant\pi/K$, and then we compute the first L Fourier harmonics for Eqs. (A4) and (A5). We have taken L in the range 10–40, and we have mixed 5–10 Landau levels. Then, we use Eqs. (3.12) and (3.13) to calculate the conductivity tensor.

In order to resolve both the van Hove peaks in the modulated system and the spin splitting of the Landau bands, we need a very small disorder parameter. In Fig. 5 we show the magnetoconductivity tensor for a magnetic field B_0 varied such that the Fermi level traverses the Landau bands with $n=1$ and 2. In Fig. 5(a) we consider a pure electric modulation of amplitude $V=15$ meV and period $a=500$ nm. For a better understanding of the conductivity oscillations, three qualitatively different energy-band structures are indicated in Fig. 6, in a half Brillouin zone. The bands corresponding to opposite spin directions are separated for filling factors below 4, i.e., for $B_0>2.5$ T, due to the exchange enhancement, and they partially overlap for higher filling factors.

For the electric modulation the energy dispersion is strongly dependent on $D(E_F)$, due to the strong screening contained both in $\Sigma^{\text{ee},H}$ and in $\Sigma^{\text{ee},F}$. All the Landau bands shrink whenever a band is intersected by the Fermi level. Therefore a full spin splitting—i.e., nonoverlapping bands with the same n, but with different spin directions—can result even for a modulation amplitude much larger than $\hbar\omega_c$.

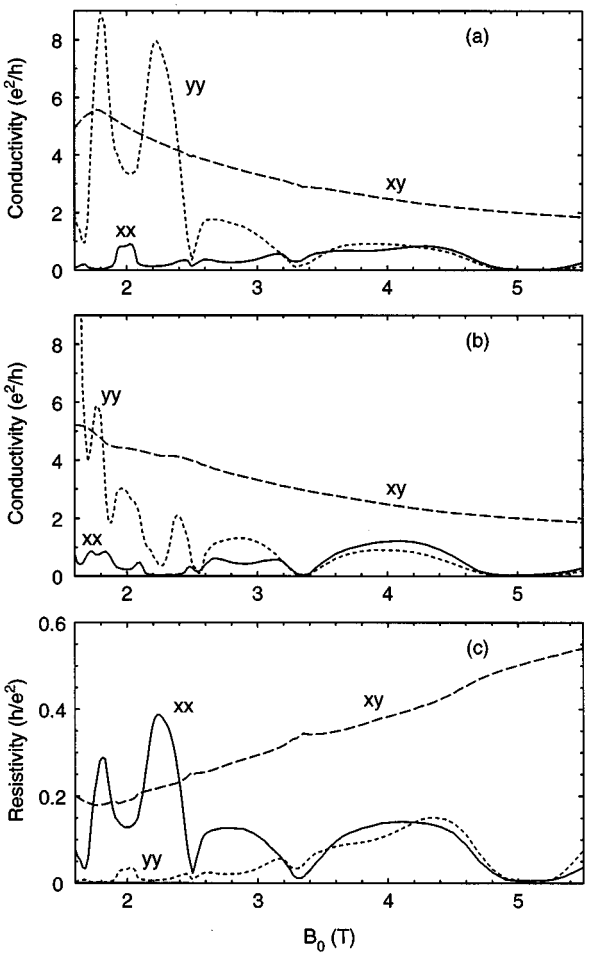

FIG. 5. The conductivity tensor calculated for (a) an electric modulation with $a=500$ nm and $V=15$ meV, (b) a magnetic modulation with $a=500$ nm and $B_1=0.25$ T, and (c) the resistivities corresponding to (a). The xx components are magnified by a factor of 2. The temperature $T=1$ K and the disorder parameter $\gamma=0.06$.

Due to the small bandwidth, and also due to the pinning of the band edges to the Fermi level, the resolution of the vHS peaks requires a very small disorder broadening. For our parameters the vHS's can be distinguished in σ_{xx}, Fig. 5, and their resolution even improves with decreasing magnetic field. The reason is the increase of the exchange interaction, self-consistently with the reduction of the DOS: $D(E_F)$ decreases, the screening diminishes, and the exchange broadening is larger. Nevertheless, the screening may again increase for overlapping bands, like in Fig. 6(c). In that case two bands contribute to the pinning effect, and therefore the resolution of the vHS's in the states $(2,+,0)$ and $(2,-,\pi/K)$, which yield the two maxima of σ_{xx} in Fig. 5(a) for $1.9\ \mathrm{T}<B_0<2.1$ T, is poorer than in the states $(2,+,\pi/K)$ and $(2,-,0)$, that is for $2.4\ \mathrm{T}<B_0<2.5$ T and $1.6\ \mathrm{T}<B_0<1.7$ T, respectively.

While the scattering component of σ_{yy} is nearly identical to σ_{xx}, the very small disorder parameter makes the band conductivity large. In Fig. 5(a), σ_{yy} is thus in the situation depicted in Fig. 4(c), with the vHS profile hidden by the band-conductivity single peak. Decreasing the magnetic field, due to the stronger energy dispersion the band conductivity further increases, contrary to the scattering term, which becomes negligible. For the overlapping bands of Fig. 6(c), the minimum of σ_{yy} at $B_0=2$ T corresponds to the strongest screening, i.e., to the highest $D(E_F)$.

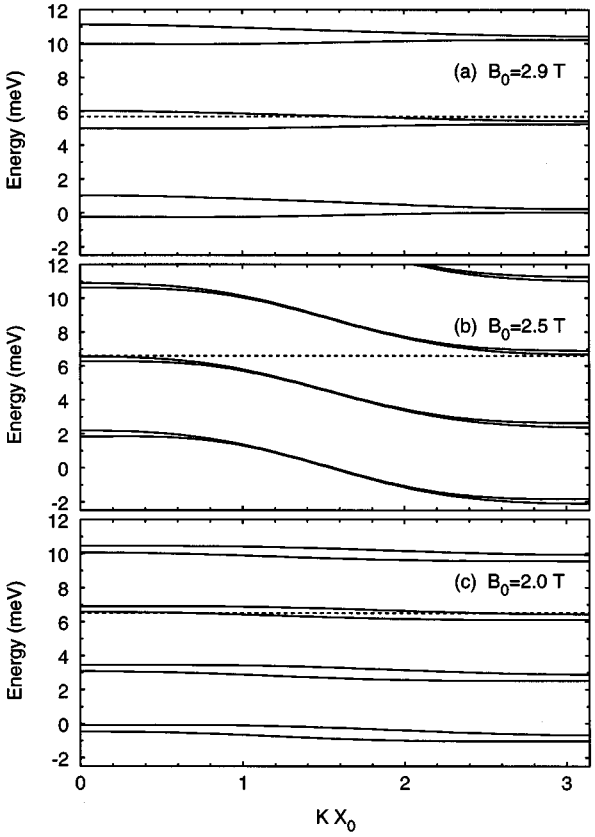

FIG. 6. Three energy spectra corresponding to Fig. 5(a).

In Fig. 5(b) we show similar results obtained for a purely magnetic modulation which produces Landau bands equivalent to those of Fig. 6. We have chosen $B_1=0.25$ T, the other parameters of the calculation being the same as those for Fig. 5(a). There are two, but unessential differences with respect to the electric modulation of Fig. 5(a). First, the energy dispersion increases with increasing Landau quantum number n. In a crude approximation, i.e., neglecting the Coulombian effects, as long as $Kl\ll 1$ the energy bands are determined by the local cyclotron energy, $E_{n\sigma X_0}=(\hbar e/m^*)\times(B_0+B_1\cos KX_0)(n+\frac{1}{2})$. Second, as mentioned at the end of Sec. II, the Hartree (direct) screening is weaker than in the electric case, and hence the strength of the exchange with respect to the Hartree interaction may increase to some extent. Going through Fig. 5(b) from high to low values of the constant field B_0, the increase of the energy dispersion at the Fermi level due to the increase of the quantum number n is thus amplified by the exchange broadening. For filling factors higher than 4, four Landau bands overlap, i.e., those with $n=2$ and 3. The order of the vHS's observed in σ_{xx}, for $B_0<2.5$ T is $(2,+,\pi/K)$ $(B_0=2.48\ \mathrm{T})$, $(2,-,\pi/K)$ $(B_0=2.10\ \mathrm{T})$, $(2,+,0)$ $(B_0=1.84\ \mathrm{T})$, and $(3,+,\pi/K)$ $(B_0=1.72\ \mathrm{T})$. The small scattering conductivity σ_{xx} for $2.15\ \mathrm{T}<B<2.40$ T also reflects a strong energy dispersion. Additionally, the screening-exchange balance may generate weak DOS fluctuations near the band edges,[8] which can be

seen as the shoulders of the band conductivity (via the Green function squared in the Kubo formula), in σ_{yy} for $2.0\ \mathrm{T} < B_0 < 2.5\ \mathrm{T}$. For lower magnetic fields, when $D(E_F)$ increases due to the overlapping bands, the exchange effects are again small, and the maxima of the scattering conductivity corresponds to the minima of the band conductivity, and vice versa.

For comparison with experiment we need to invert the conductivity tensor into resistivities,

$$\rho_{xx}=\frac{\sigma_{yy}}{\mathcal{D}}, \quad \rho_{yy}=\frac{\sigma_{xx}}{\mathcal{D}}, \quad \rho_{xy}=\frac{\sigma_{yx}}{\mathcal{D}}, \tag{4.1}$$

where $\mathcal{D}=\sigma_{xx}\sigma_{yy}+\sigma_{xy}^2$. In our calculations $\sigma_{xx}\sigma_{yy} \ll \sigma_{xy}^2$, and hence we have $\rho_{xx,yy} \approx \sigma_{yy,xx}/\sigma_{xy}^2$. In Fig. 5(c) we see that the resistivity measured perpendicular to the modulation reflects in fact the band conductivity, while the scattering conductivity alone can be observed only in the resistivity measured parallel to the modulation.

In the experiments on the systems with an etched electric modulation, of parameters comparable to our model, more complicated structures of the resistivity ρ_{xx} have been observed.[8] The SdH maxima corresponding to a certain spin direction may show two and even three internal peaks. One possible explanation could consist in the more complicated exchange effects on the band conductivity, like the shoulders we have found for the magnetic modulation, Fig. 5(b). We have also obtained such effects for an electric modulation, with a shorter period, $a=100$ nm, when the screening is considerably reduced.[8] Another possible explanation, which is supported by the present results of the SHFA, is that in the real system the band and the scattering conductivities may be comparable in magnitude, such that their superposition in σ_{yy} may lead to one to three peaks per Landau level, as illustrated in Fig. 4. However, within our approximations, the price for the resolution of both the spin splitting and the vHS's is a relatively large band conductivity.

To our knowledge, a simultaneous measurement of both ρ_{xx} and ρ_{yy}, capable of indicating the real magnitude of the two components of the longitudinal conductivities, has been reported, at high magnetic fields, only for the short-period modulated systems,[10] and ρ_{xx} has been found considerably larger than ρ_{yy}, but without a clear DOS structure. For short periods, the Hartree screening becomes weaker, and the Landau bands become wider, such that in principle we could cover several situations, including those of Fig. 4, by varying the modulation amplitude and the disorder parameter γ. We cannot extend our SHFA to that regime, because of the steepness of the energy dispersion which is not compatible with the assumption about the quasihomogeneous screening of the exchange interaction. Nevertheless, the results of the HFA may be satisfactory.[8]

We want now to discuss the situation of an electric modulation with a larger amplitude, such that the Landau bands overlap. In the experiment by Weiss *et al.*,[7] the double-peak structure of the resistivity ρ_{xx} has been found, while the absence of the spin splitting for the unmodulated system may be attributed to the combined disorder and thermal effects. We have recently confirmed such a possibility, within the SHFA, by choosing such a disorder parameter and temperature that both the exchange enhancement of the Zeeman

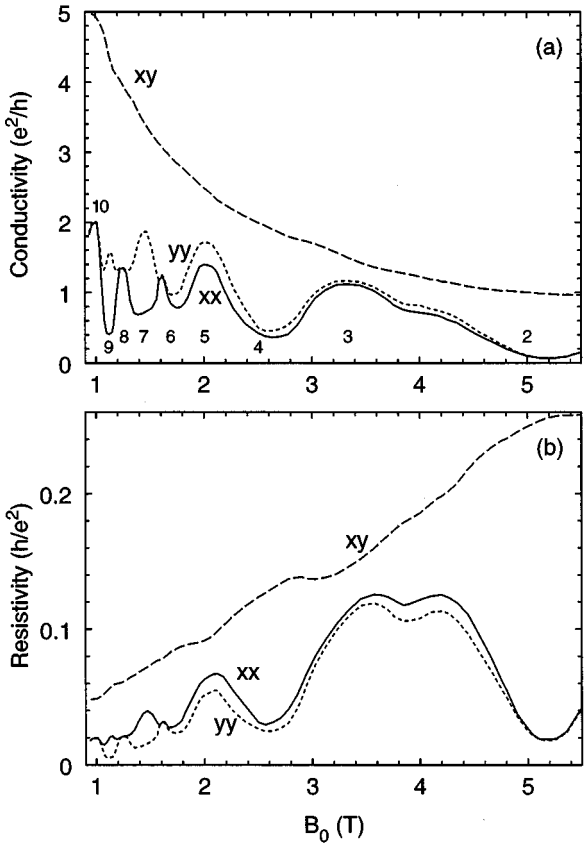

FIG. 7. (a) The conductivities and (b) the resistivities, for an electric modulation with $a=500$ nm and $V=20$ meV. The Hall components are reduced by a factor of 2. The numbers inside the plot indicate the filling factors. $T=1$ K and $\gamma=0.20$.

splitting and the band conductivity have been suppressed, and ρ_{xx} have been obtained as resulting from Fig. 4(a).[24]

In the example of Fig. 7 we consider the situation in which neither the spin splitting nor the vHS's are resolved in the low-energy Landau bands, but the vHS's develop in the higher, overlapped bands. The SdH minima at filling factors around 2 and 4 are slightly shifted to higher magnetic fields. The energy gaps are small, nearly vanishing, but the adjacent bands are separated due to the pinning effect. For weaker magnetic fields, at even filling factors the vHS's from the top of the Landau band below the Fermi level overlaps with that from the bottom of the upper band, resulting in the maxima of σ_{xx} for $\nu=8$ and 10 and in the minima for the odd filling factors $\nu=7$ and 9. The transition occurs around $\nu=6$. Since the DOS decreases when the magnetic field is lowered, the screening becomes less efficient, and the bandwidth may increase when the Fermi level is in a band center, leading to a large band conductivity, wherefrom the maxima of σ_{yy} for $\nu=7$ and 9. The switching from even to odd filling factors at the resistivity minima, which we show here only for ρ_{yy} (σ_{xx}), has been recently observed for ρ_{xx} and supported by a transport calculation similar to the present one, but with the Coulomb interaction neglected.[9]

Finally we want to mention that the plateaus we obtain for the Hall resistivity, Fig. 7(b), do not correspond to plateaus of the Hall conductivity, since localization effects do not exist in our model, but to the wide minima of the longitudi-

nal conductivities. In the noninteracting approximation, and also in the HFA, for a fixed number of particles, the Fermi level jumps abruptly from one Landau band to the other. In the SHFA the exchange interaction is very sensitive to the variation of $D(E_F)$, and since they are self-consistently determined, the stability of the chemical potential in an energy gap considerably improves.

V. CONCLUSIONS AND FINAL REMARKS

We have calculated energy spectra of a two-dimensional electron gas in an electric or magnetic superlattice, and in a perpendicular magnetic field, beyond the standard HFA. The superlattice potential is smooth and the uniform magnetic field is strong, such that the electrostatic screening is very important. The essential element of our approach is the inclusion of screening in the exchange term, self-consistently with the DOS at the Fermi level. The numerical calculations are complicated and time consuming, such that approximations in treating the screening are unavoidable: we have only considered the static screening, in a manner appropriate to a quasihomogeneous system. Improvements of our procedure are possible, e.g., along the lines of Refs. 32 and 33, but even within the present approach the results drastically change with respect to the HFA. The obtained screening of the exchange interaction may be even somewhat too strong, since we found that our SHFA yields no charge-density-wave instability of the homogeneous 2DEG, even at very low filling factors.

Using a large-amplitude modulation as a model for edge states, we have shown that our SHFA results interpolate between the contradictory Hartree and Hartree-Fock approximations: we obtained both compressible edge strips much wider than the magnetic length, and an enhanced spin splitting. To the best of our knowledge, this expected result has never been obtained within a microscopic many-body theory before.

For a weak modulation, the standard HFA yields strong short-range oscillations of the Landau bands and the particle density, which to our knowledge have never been observed experimentally. Such oscillations completely disappear in our SHFA, and we believe that these present results are much more realistic. Clearly, we cannot expect a quantitative agreement with experiments since, besides the approximations regarding the electron-electron interaction, we have used a rather crude simplification of the electron-impurity scattering in our transport calculation, such that the disorder vertex correction vanishes. However, qualitatively, we have obtained smooth internal structures of the SdH peaks determined by the interplay of the scattering and band conductivities, the ingredients of which have been carefully analyzed. These smooth internal structures compare much more favorably with the experimental results than the sharp structures near the Landau band edges obtained in the bare HFA.[8]

ACKNOWLEDGMENTS

We wish to thank Marc Tornow, Dieter Weiss, Behnam Farid, and Paul Gartner for discussions. One of us (A.M.) is also grateful to the Max-Planck-Institut für Festkörperforschung, Stuttgart, for support and hospitality.

APPENDIX A: HAMILTONIAN MATRIX ELEMENTS

With the notations $z=(Kl)^2/2$ and

$$F_{nn'}(z)=\left(\frac{n'!}{n!}\right)^{1/2} z^{(n-n')/2}e^{-z/2}L_{n'}^{n-n'}(z), \tag{A1}$$

where $L_{n'}^{n-n'}(z)$ are the Laguerre polynomials,[37] $n,n'=0,1,\ldots$, and $F_{nn'}=(-1)^{n-n'}F_{n'n}$, we can write the matrix elements of the noninteracting Hamiltonian in the form

$$\begin{aligned}H^0_{nn'}(\sigma,X_0)=&\,\delta_{nn'}\hbar\omega_c\left[n+\frac{1}{2}+\frac{1}{8z}\left(\frac{B_1}{B_0}\right)^2\right]-\delta_{nn'}\frac{\sigma}{2}g\mu_B B_0\\&+\left[\frac{\hbar\omega_c}{2z}\frac{B_1}{B_0}[F_{nn'}(z)+\sqrt{nn'}F_{n-1,n'-1}(z)\right.\\&-\sqrt{(n+1)(n'+1)}F_{n+1,n'+1}(z)]\\&\left.+\left(V-\frac{\sigma}{2}g\mu_B B_1\right)F_{nn'}(z)\right]\\&\times\cos\left(KX_0+(n-n')\frac{\pi}{2}\right)\\&-\frac{\hbar\omega_c}{8z}\left(\frac{B_1}{B_0}\right)^2F_{nn'}(4z)\\&\times\cos\left(2KX_0+(n-n')\frac{\pi}{2}\right).\end{aligned} \tag{A2}$$

Due to the reflection symmetry of the external fields, we have the parity rule

$$H^0_{nn'}(\sigma,X_0)=(-1)^{n-n'}H^0_{nn'}(\sigma,-X_0), \tag{A3}$$

which also holds for the Coulomb self-energy matrix elements, Eq. (2.9), which depend on the self-consistent wave functions given by Eq. (2.4). In order to write those matrix elements in a form suitable for a numerical calculation, we expand the mixing coefficients in Fourier series,

$$c_{nn'}(\sigma,X_0)=\sum_{p\geqslant 0}\gamma_{nn'}(\sigma,p)\cos\left(pKX_0+(n-n')\frac{\pi}{2}\right), \tag{A4}$$

where we have taken into account the parity rule.

The effective energies can thus be expanded as

$$E_{n\sigma X_0}=\sum_{p\geqslant 0}\epsilon_{n\sigma p}\cos pKX_0, \tag{A5}$$

and similarly the occupation numbers

$$\nu_{n\sigma X_0}=\sum_{p\geqslant 0}f_{n\sigma p}\cos pKX_0. \tag{A6}$$

We define

$$A^{n_1n_2n_3n_4}_{p_1p_2p_3p_4}=\frac{4}{\pi}\int_{-\pi}^{\pi}dx\prod_{i=1}^{4}\cos\left(p_ix+n_i\frac{\pi}{2}\right). \tag{A7}$$

With this notation, and using Eqs. (A4) and (A6), the Fourier coefficients of the particle density can be written, by inverting Eq. (2.10), as

$$n_p=\frac{2-\delta_{p0}}{16\pi l^2}\sum_{\substack{m_1\geqslant 0,\sigma=\pm\\ p_1\geqslant 0}} f_{m_1\sigma p_1}\times\sum_{\substack{m_2,m_3\geqslant 0\\ p_2,p_3\geqslant 0}} A_{pp_1p_2p_3}^{m_2-m_3,0,m_1-m_2,m_1-m_3}\times F_{m_2m_3}(p^2z)\,\gamma_{m_1m_2}(\sigma,p_2)\,\gamma_{m_1m_3}(\sigma,p_3). \quad \text{(A8)}$$

The matrix elements of the Hartree term, defined by Eqs. (2.9) and (2.10), can now be put in the form

$$\Sigma_{nn'}^{\mathrm{ee},H}(X_0)=\frac{2\pi e^2}{\kappa Kl}\sum_{p\geqslant 1}\frac{n_p}{p}F_{nn'}(p^2z)\times\cos\left(pKX_0+(n-n')\,\frac{\pi}{2}\right), \quad \text{(A9)}$$

where we have used the Fourier transform of the Coulomb potential. The corresponding Fourier series for the Fock term of the Hamiltonian, Eq. (2.11), can be found by directly searching for the Fourier amplitudes, and, after a lengthy, but straightforward calculation, one obtains

$$\Sigma_{nn'}^{\mathrm{ee},F}(\sigma,X_0)=-\frac{1}{16\pi^2 l}\sum_{p\geqslant 0}(2-\delta_{p0})\times\cos\left(pKX_0+(n-n')\,\frac{\pi}{2}\right)\sum_{\substack{m_1\geqslant 0\\ p_1\geqslant 0}} f_{m_1\sigma p_1}\times\sum_{\substack{m_2,m_3\geqslant 0\\ p_2,p_3\geqslant 0}} A_{pp_1p_2p_3}^{m_2-m_3,0,m_1-m_2,m_1-m_3}\times S_{nm_2,n'm_3}(pKl)\,\gamma_{m_1m_2}(\sigma,p_2)\,\gamma_{m_1m_3}(\sigma,p_3), \quad \text{(A10)}$$

where S denotes the exchange integrals

$$S_{m_1n_1,m_2n_2}(t)=\left(\frac{m_1!m_2!}{n_1!n_2!}\right)^{1/2}\int_0^\infty dq\,\tilde{u}(q\sqrt{2})e^{-q^2}\times q^{n_1-m_1+n_2-m_2+1}J_{n_1-m_1-n_2+m_2}(tq\sqrt{2})\times L_{m_1}^{n_1-m_1}(q^2)L_{m_2}^{n_2-m_2}(q^2), \quad \text{(A11)}$$

with $J_n(x)$ the Bessel functions. For the homogeneous system the self-consistent wave functions are identical with the Landau wave functions, so that $\gamma_{n_1n_2}(\sigma,p)=\delta_{n_1n_2}\delta_{p0}$, and the exchange integrals reduce to $S_{m_1n_1,m_1n_1}(0)$.[14,28]

APPENDIX B: VELOCITY MATRIX ELEMENTS

The matrix elements of the noninteracting components of the velocity operators, Eq. (3.5), in the absence of a magnetic modulation, are

$$(v_\alpha^0)_{nn'}(X_0)=\eta_\alpha\frac{l\omega_c}{\sqrt{2}}(\sqrt{n+1}\,\delta_{n',n+1}+\eta_\alpha^2\sqrt{n'+1}\,\delta_{n,n'+1}), \quad \text{(B1)}$$

with the notation $(\eta_x,\eta_y)=(i,1)$. When the magnetic field has a periodic component in the x direction, one has to add to v_y^0 the extra term

$$\frac{\omega_c B_1}{KB_0}F_{nn'}(z)\sin\left(KX_0+(n-n')\,\frac{\pi}{2}\right). \quad \text{(B2)}$$

The matrix elements of the exchange current can be transformed in Fourier series like those of the exchange-interaction operator, as sketched in Appendix A. According to Eq. (3.6), the form of $\mathbf{v}_{nn'}^{\mathrm{ex}}(\sigma,X_0)$ is similar to that of $\Sigma_{nn'}^{\mathrm{ee},F}(\sigma,X_0)$, with the replacement $u(\mathbf{r}-\mathbf{r}')\to(\mathbf{r}-\mathbf{r}')\times u(\mathbf{r}-\mathbf{r}')$ in Eq. (2.9), and, after an integration by parts, with $\tilde{u}(\mathbf{q})\to\nabla_{\mathbf{q}}\tilde{u}(\mathbf{q})$ in Eq. (2.11), one obtains the following Fourier expansion:

$$\mathbf{v}_{nn'}^{\mathrm{ex}}(\sigma,X_0)=\frac{1}{8\sqrt{2}\pi h}\sum_{p\geqslant 0}(2-\delta_{p0})\times\sin\left(pKX_0+(n-n')\,\frac{\pi}{2}\right)\times\sum_{\substack{m_1\geqslant 0\\ p_1\geqslant 0}} f_{m_1\sigma p_1}\sum_{\substack{m_2,m_3\geqslant 0\\ p_2,p_3\geqslant 0}}\times A_{pp_1p_2p_3}^{m_2-m_3,0,m_1-m_2,m_1-m_3}\mathbf{T}_{nm_2,n'm_3}(pKl)\times\gamma_{m_1m_2}(\sigma,p_2)\,\gamma_{m_1m_3}(\sigma,p_3), \quad \text{(B3)}$$

in which

$$(T_\alpha)_{m_1n_1,m_2n_2}(t)=\eta_\alpha\left(\frac{m_1!m_2!}{n_1!n_2!}\right)^{1/2}\int_0^\infty dq\left[\frac{d\tilde{u}(q\sqrt{2})}{dq}\right]\times e^{-q^2}q^{n_1-m_1+n_2-m_2+1}[J_{n_1-m_1-n_2+m_2-1}(tq\sqrt{2})-\eta_\alpha^2 J_{n_1-m_1-n_2+m_2+1}(tq\sqrt{2})]\times L_{m_1}^{n_1-m_1}(q^2)L_{m_2}^{n_2-m_2}(q^2). \quad \text{(B4)}$$

[1] D. Weiss, K. v. Klitzing, K. Ploog, and G. Weimann, Europhys. Lett. **8**, 179 (1989).
[2] H. A. Carmona *et al.*, Phys. Rev. Lett. **74**, 3009 (1995).
[3] P. D. Ye *et al.*, Phys. Rev. Lett. **74**, 3013 (1995).
[4] F. M. Peeters and P. Vasilopoulos, Phys. Rev. B **47**, 1466 (1993); P. Vasilopoulos and F. M. Peeters, Superlattices Microstruct. **7**, 393 (1990).
[5] For a recent review, see R. R. Gerhardts, Phys. Rev. B **53**, 11 064 (1996).
[6] T. Schlösser, K. Ensslin, J. P. Kotthaus, and M. Holland, Europhys. Lett. **33**, 683 (1996).
[7] D. Weiss, K. v. Klitzing, K. Ploog, and G. Weimann, Surf. Sci. **229**, 88 (1990).
[8] A. Manolescu, R. R. Gerhardts, M. Tornow, D. Weiss, K. v. Klitzing, and G. Weimann, Surf. Sci. **361/362**, 513 (1996).
[9] M. Tornow, D. Weiss, A. Manolescu, R. Menne, K. v. Klitzing, and G. Weimann, Phys. Rev. B **54**, 16 397 (1996).
[10] L. Sfaxi, F. Petit, F. Lelarge, A. Cavanna, and B. Etienne, Surf. Sci. **361/362**, 860 (1996).
[11] F. Petit, L. Sfaxi, F. Lelarge, A. Cavanna, M. Hayne, and B. Etienne, Europhys. Lett. **38**, 225 (1997).
[12] G. R. Aizin and V. A. Volkov, Zh. Eksp. Teor. Fiz. **87**, 1469 (1984) [Sov. Phys. JETP **60**, 844 (1984)].
[13] C. Zhang and R. R. Gerhardts, Phys. Rev. B **41**, 12 850 (1990).
[14] A. Manolescu and R. R. Gerhardts, Phys. Rev. B **51**, 1703 (1995).
[15] A. Manolescu, Phys. Rev. B **52**, 2831 (1995).
[16] H. Fukuyama, P. M. Platzman, and P. W. Anderson, Phys. Rev. B **19**, 5211 (1979).
[17] D. B. Chklovskii, B. I. Shklovskii, and L. I. Glazman, Phys. Rev. B **46**, 4026 (1992).
[18] L. Brey, J. J. Palacios, and C. Tejedor, Phys. Rev. B **47**, 13 884 (1993).
[19] K. Lier and R. R. Gerhardts, Phys. Rev. B **50**, 7757 (1994).
[20] J. Dempsey, B. Y. Gelfand, and B. I. Halperin, Phys. Rev. Lett. **70**, 3639 (1993).
[21] L. Rijkels and G. E. W. Bauer, Phys. Rev. B **50**, 8629 (1994).
[22] T. H. Stoof and G. E. W. Bauer, Phys. Rev. B **52**, 12 143 (1995).
[23] N. B. Zhitenev, R. J. Haug, K. v. Klitzing, and K. Eberl, Phys. Rev. Lett. **71**, 2292 (1993).
[24] A. Manolescu and R. R. Gerhardts (unpublished).
[25] U. Wulf, V. Gudmundsson, and R. R. Gerhardts, Phys. Rev. B **38**, 4218 (1988).
[26] P. D. Ye and D. Weiss (private communication).
[27] A. L. Fetter and J. D. Walecka, *Quantum Theory of Many-Particle Systems* (McGraw-Hill, New York, 1971).
[28] For a similar treatment of the homogeneous 2DEG, see A. H. MacDonald, H. C. A. Oji, and K. L. Liu, Phys. Rev. B **34**, 2681 (1986).
[29] V. Gudmundsson and R. R. Gerhardts, Solid State Commun. **67**, 845 (1988).
[30] J. Labbé, Phys. Rev. B **35**, 1373 (1987).
[31] T. Ando and Y. Uemura, J. Phys. Soc. Jpn. **37**, 1044 (1974).
[32] F. J. Ohkawa and Y. Uemura, J. Phys. Soc. Jpn. **43**, 925 (1977).
[33] S. Katayama and T. Ando, Solid State Commun. **70**, 97 (1989).
[34] T. Uenoyama and L. J. Sham, Phys. Rev. B **39**, 11 044 (1989).
[35] U. J. Gossmann, A. Manolescu, and R. R. Gerhardts (unpublished).
[36] R. R. Gerhardts, Z. Phys. B **22**, 327 (1975), and references therein.
[37] Strictly speaking $L_n^k(x)$ are defined only for $k>-1$, see, e.g., *Handbook of Mathematical Functions*, edited by M. Abramowitz and I. A. Stegun (Dover, New York, 1972). However, for integer k, $0<k\leqslant n$, one can formally write $L_n^{-k}(x)=(-1)^k[(n-k)!/n!]\,x^k L_{n-k}^k(x)$.